



AD FALCON API Manual

Mohr–Coulomb Plasticity (Rounded)

Javad Ghorbani

March 26, 2026

Contents

1	Mohr–Coulomb Plasticity (Rounded)	3
1.1	Syntax	3
1.2	Material parameters	3
1.3	Effective stress for unsaturated soils	4
1.3.1	Enriched $\chi(S_w)$ (near-dry attenuation)	4
1.4	Stress invariants	5
1.5	Smooth Mohr–Coulomb yield (Abbo–Sloan)	5
1.5.1	Rounding parameter and transition angle	6
1.6	Plastic potential (non-associated)	6
1.6.1	Optional dilatancy cap (DilatationPvCap)	7
1.7	Elastic law	7
1.8	FALCON mini	8
1.8.1	How to run	8
1.8.2	Input syntax	8
1.8.3	Hydromechanical assumptions	12
1.8.4	Sample input	12
1.8.5	Output files and columns	16
1.9	Results	17
1.9.1	Drained reference case	17
1.9.2	Undrained reference case	17
1.9.3	Unsaturated companion cases	19
1.10	Applications and limitations	20
1.11	References (selection)	20

1 Mohr–Coulomb Plasticity (Rounded)

Mohr–Coulomb plasticity with the smooth Abbo–Sloan hyperbolic approximation.

1.1 Syntax

This model is configured in % `Materials` as a user-defined mechanical material. Use `@UMAT:` with category `Mechanical` and pass the parameters as `name=value` pairs.

Example:

```
@UMAT: path/to/mohr.cpp path/to/mohr.hpp Mechanical E=1e8 Nu=0.3 Phi=30
Cohesion=10e3 Psi=0
```

Optional parameters:

- `DilationPvCap` (dilatancy cap): caps the accumulated plastic volumetric strain at which dilatancy is switched off (omit it, or set it ≤ 0 , to disable).

Example with a dilatancy cap:

```
@UMAT: path/to/mohr.cpp path/to/mohr.hpp Mechanical E=1e8 Nu=0.3 Phi=30
Cohesion=10e3 Psi=10 DilationPvCap=0.02
```

Use the parameter names shown in the table below.

1.2 Material parameters

Symbol	Keyword in input	Units	Required	Description
E	<code>E</code>	stress	✓	Young's modulus.
ν	<code>Nu</code>	–	✓	Poisson's ratio.
ϕ'	<code>Phi</code>	°	✓	Friction angle (effective stress).
c'	<code>Cohesion</code>	stress	✓	Cohesion (effective stress).
ψ	<code>Psi</code>	°	✓	Dilatancy angle for non-associated flow.
a	<code>RoundingParam</code>	–	✓	Hyperbolic rounding parameter.

Symbol	Keyword in input	Units	Required	Description
STOL	STOL	–	✓	Stress integration tolerance.
FTOL	FTOL	–	✓	Yield-surface tolerance.
$\varepsilon_v^{p, cap}$	DilationPvCap	strain	×	Optional cap on the accumulated plastic volumetric strain (positive in tension) at which the dilatancy angle is set to zero (disabled if ≤ 0).



1.3 Effective stress for unsaturated soils

Let the **net stress** and **matric suction** be

$$\sigma_{\text{net}} = \sigma + p_a \mathbf{I}, \quad s = p_a - p_w$$

With Bishop-type weighting $\chi \in [0, 1]$, the **effective stress** used throughout the model is

$$\sigma' = \sigma_{\text{net}} - \chi s \mathbf{I} \quad (1)$$

so that suction contributes to strength through the **suction stress** $\sigma_{\text{suc}} = \chi s$. This recovers the familiar saturated and dry limits and is the basis for calibration from shear tests.

1.3.1 Enriched $\chi(S_w)$ (near-dry attenuation)

To capture the observed **peak and attenuation** of suction-driven strength toward the dry end, χ is enriched as a **multiplicative function of degree of saturation** S_w . The Ghorbani and Kodikara (2024) formulation provides a flexible representation, and its implications for unsaturated Mohr-Coulomb bearing-capacity problems are discussed further by Ghorbani et al. (2026):

$$\chi(S_w) = S_w^{\left(\frac{\beta_1}{S_w^{\beta_2}}\right)} \quad (2)$$

with two material parameters (β_1, β_2) controlling the shape. This preserves $\chi \rightarrow 0$ as $S_w \rightarrow 0$ and $\chi \rightarrow 1$ as $S_w \rightarrow 1$, while allowing a tunable near-dry decay of σ_{suc} . Set $\beta_1 = 1$ and $\beta_2 = 0$ to recover the classical $\chi = S_w$ (Bishop's model).

For detailed information, see [Effective Stress Model – Ghorbani and Kodikara \(2024\)](#).

Note on coupled saturated analyses: In fully saturated coupled analyses where $S_w = 1$, the effective stress formulation reduces to Terzaghi's classical definition ($\chi = 1$), and the model operates as a standard Mohr–Coulomb plasticity in terms of effective stress. See [Coupled Analysis](#) for details on saturated formulations.

1.4 Stress invariants

Mean effective stress p (compression positive in geomechanics; here **remember stresses are tension-positive**, so $p = -\sigma_m$ if you prefer compression-positive):

$$\sigma_m = \frac{1}{3} \text{tr } \boldsymbol{\sigma}', \quad \mathbf{s} = \boldsymbol{\sigma}' - \sigma_m \mathbf{I}, \quad J_2 = \frac{1}{2} \mathbf{s} : \mathbf{s}, \quad J_3 = \det(\mathbf{s}), \quad \theta = \frac{1}{3} \arcsin\left(-\frac{4.5 J_3}{\sqrt{3} J_2^{3/2}}\right)$$

1.5 Smooth Mohr–Coulomb yield (Abbo–Sloan)

The classical Mohr–Coulomb criterion exhibits singular corners on the deviatoric plane. To enable robust numerical integration, we adopt the **hyperbolic smooth approximation** proposed by Abbo and Sloan (1995), which effectively rounds these angular corners while maintaining close fidelity to the original hexagonal surface. The yield function is expressed in stress invariants as:

$$f(\boldsymbol{\sigma}') = \sqrt{J_2} K(\theta) + \sigma_m \sin \phi' - c' \cos \phi' = 0 \quad (3)$$

where:

- ϕ' is the friction angle
- c' is the cohesion
- θ is the **Lode angle**, defined as

$$\theta = \frac{1}{3} \sin^{-1}\left(-\frac{3\sqrt{3}}{2} \frac{J_3}{J_2^{3/2}}\right)$$

The function $K(\theta)$ is defined **piecewise** to blend two hyperbolic branches across a **transition angle** θ_T :

$$K(\theta) = \begin{cases} A - B \sin(3\theta) & \text{if } |\theta| > \theta_T \\ \cos \theta - \frac{1}{\sqrt{3}} \sin \theta \sin \phi' & \text{if } |\theta| \leq \theta_T \end{cases} \quad (4)$$

with parameters:

$$A = \frac{1}{3} \cos \theta_T \left(3 + \tan \theta_T \tan(3\theta_T) + (\tan(3\theta_T) - 3 \tan \theta_T) \frac{1}{\sqrt{3}} \sin \phi' \sin \phi' \right) \quad (5)$$

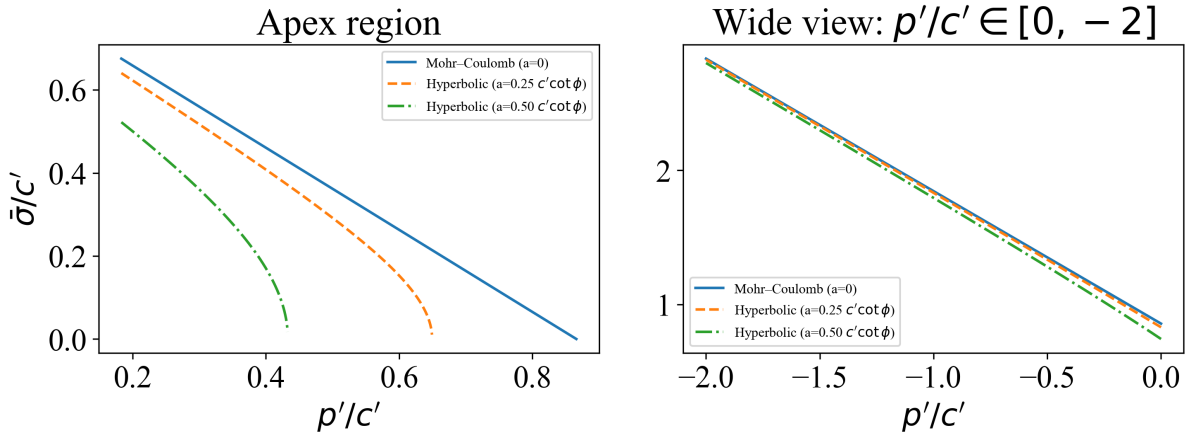


Figure 1: Effect of apex smoothing on the Mohr-Coulomb yield surface

$$B = \frac{1}{3 \cos(3\theta_T)} \left(\sin \theta \sin \theta_T + \frac{1}{\sqrt{3}} \cos \theta \sin \phi' \right) \quad (6)$$

1.5.1 Rounding parameter and transition angle

The **rounding parameter** a controls how closely the smooth surface matches the exact Mohr-Coulomb hexagon:

- For $a \leq 0.25$, the approximation is nearly indistinguishable from the original M-C surface, but $\cot \phi'$ must be small to avoid numerical ill-conditioning.
- As $a \rightarrow 0$, the hyperbolic surface converges to the hexagonal M-C criterion with sharp corners.
- A typical choice is $a \approx 0.05 \cot \phi'$, balancing accuracy with numerical stability.

The **transition angle** θ_T is selected slightly below the M-C corner angle to ensure smooth blending and avoid singularities near the corners. In FALCON, θ_T is set to a default value of **29.5°** and is not user-adjustable.

Note: In principal stress space, this formulation recovers the familiar triaxial compression and extension meridians. The smooth approximation removes apex and edge singularities, enabling consistent tangent operators for implicit stress integration.

Figure 1.: The hyperbolic smoothing adopted in FALCON.

1.6 Plastic potential (non-associated)

Non-associated flow uses the same structure with the **dilatancy** ψ angle replacing the friction angle.

1.6.1 Optional dilatancy cap (DilationPvCap)

To prevent unbounded volumetric expansion in highly dilatant materials, an optional cap can be applied to the accumulated plastic volumetric strain (positive in tension):

- Define `DilationPvCap > 0` to activate. If omitted or set ≤ 0 , the cap is disabled and the dilatancy remains equal to the prescribed ψ .
- Let the accumulated plastic strains be $\varepsilon_{xx}^p, \varepsilon_{yy}^p, \varepsilon_{zz}^p$. The model monitors the plastic volumetric strain $\varepsilon_v^p = \varepsilon_{xx}^p + \varepsilon_{yy}^p + \varepsilon_{zz}^p$ (positive in tension). When ε_v^p reaches `DilationPvCap`, the effective dilatancy used in the plastic potential is set to zero for the remainder of the analysis (i.e., $\psi_{\text{eff}} = 0$ afterward).

Practical guidance: - Smaller caps (e.g., `DilationPvCap = 0.02`) shut off dilatancy earlier, limiting void ratio growth and peak strength from dilation. - Larger caps (e.g., `DilationPvCap = 0.05`) allow more dilation before switching to zero-dilatancy flow. - With `DilationPvCap ≤ 0`, the model behaves as standard non-associated M–C with constant ψ .

Influence on void ratio and response The following results are obtained from **saturated triaxial drained compression** tests. The test conditions are:

- **Drainage:** Fully drained (constant pore pressure, fully saturated)
- **Loading:** Axial compression with constant radial effective stress (conventional triaxial compression)
- **Initial state:** Isotropic effective stress of -50 kPa (compression), initial void ratio $e_0 = 0.35$
- **Material parameters:** $E = 100$ MPa, $\nu = 0.30$, $c' = 1$ kPa, $\phi' = 30^\circ$, $\psi = 10^\circ$
- **Loading path:** Axial strain increment $\Delta\varepsilon_{yy} = -1.0 \times 10^{-4}$ per step (compression negative), maintaining $\Delta q/\Delta p' = 3$ (constant radial stress)

Figure 2. Void ratio evolution for multiple analyses: no dilatancy ($\psi = 0$), constant dilatancy ($\psi = 10^\circ$), and capped dilatancy ($\psi = 10^\circ$ with `DilationPvCap = 0.02` and `0.05`). Smaller caps arrest dilation earlier, resulting in lower final void ratios.

Figure 3. Mechanical response comparison under the same paths. Enabling dilatancy ($\psi > 0$) increases peak strength due to volumetric expansion; applying a cap reduces that effect beyond the cap, aligning post-peak trends closer to the non-dilatant response.

1.7 Elastic law

The model uses **linear isotropic elasticity** with constant Young's modulus E and Poisson's ratio ν . The elastic bulk and shear moduli are:

$$K = \frac{E}{3(1-2\nu)} \quad (7)$$

$$G = \frac{E}{2(1+\nu)} \quad (8)$$

The elastic compliance tensor is standard:

$$\mathbf{D}^e = \begin{bmatrix} K + \frac{4}{3}G & K - \frac{2}{3}G & K - \frac{2}{3}G & 0 & 0 & 0 \\ K - \frac{2}{3}G & K + \frac{4}{3}G & K - \frac{2}{3}G & 0 & 0 & 0 \\ K - \frac{2}{3}G & K - \frac{2}{3}G & K + \frac{4}{3}G & 0 & 0 & 0 \\ 0 & 0 & 0 & G & 0 & 0 \\ 0 & 0 & 0 & 0 & G & 0 \\ 0 & 0 & 0 & 0 & 0 & G \end{bmatrix} \quad (9)$$

For plane strain (2D), the stress-strain relation reduces to a 3x3 sub-block corresponding to $[\sigma_{xx}, \sigma_{yy}, \sigma_{xy}]$ and $[\varepsilon_{xx}, \varepsilon_{yy}, \gamma_{xy}]$.

1.8 FALCON mini

The packaged mini tool id is MohrRounded. It lives under `mini_tools/MohrRounded`.

1.8.1 How to run

```
falcon --mini-root /path/to/UMATLIB_FALCON/falcon_minis --mini-tool
MohrRounded --mini-input
/path/to/UMATLIB_FALCON/falcon_minis/MohrRounded/cases/drained
```

Packaged simulation families:

- drained triaxial: [cases/drained/input.txt](#)
- undrained triaxial: [cases/undrained/input.txt](#)
- constant-suction q/p_{net} loading: [cases/qoverpnet/input.txt](#)
- constant-water-content loading: [cases/const_wcontent/input.txt](#)

1.8.2 Input syntax

`input.txt` uses whitespace-delimited Key Value pairs, one item per line, for example:

```
Mode Drained
E 10000
nu 0.30
StressXX -100
```

The main driver selector is Mode. It tells the standalone mini which loading program and hydraulic constraint to apply.

Mode value	Meaning in the standalone mini	Hydraulic assumption / constraint
Drained	Saturated drained triaxial loading. The driver applies axial strain and solves the radial strain so the lateral total stress remains constant.	No suction evolution is used in this packaged reference path.
Undrained	Saturated constant-volume triaxial loading. The driver applies axial strain with $e_{xx} = e_{zz} = -0.5 e_{yy}$.	No suction evolution is used in this packaged reference path.
QOverPnet	Unsaturated triaxial loading intended to follow an approximately constant $dq / dp_{net} = 3$ path.	Suction is held constant during loading. In the packaged example, $p_a = 0$ is used as the atmospheric reference and suction is therefore set through $u_w < 0$. Saturation-dependent effective stress remains active through $\chi(S_w)$.
ConstWContent	Triaxial loading with the same mechanical target family but with hydraulic evolution solved together with the stress path.	Water content is held constant, so suction, saturation, and void ratio evolve together during loading. In the packaged examples, $p_a = 0$ is used as the atmospheric reference and suction is introduced through $u_w < 0$.

Mini inputs used by the packaged cases:

Input key	Used by	Required / choices / defaults	Meaning
Mode	all cases	Required; choices Drained, Undrained, QOverPnet, ConstWContent	Selects the loading program executed by the standalone driver.

Input key	Used by	Required / choices / defaults	Meaning
E	all cases	Required in packaged cases	Young's modulus for the linear elastic part of the Mohr-Coulomb model.
nu	all cases	Required in packaged cases	Poisson's ratio for the elastic law.
Cohesion	all cases	Required in packaged cases	Mohr-Coulomb cohesion intercept.
FrictionAngle	all cases	Required in packaged cases	Friction angle in degrees.
DilationAngle	all cases	Required in packaged cases	Plastic dilation angle in degrees.
Rf	all cases	Required in packaged cases	Abbo-Sloan rounding parameter controlling how sharp the rounded Mohr-Coulomb surface remains.
STOL	all cases	Optional; UMAT default if omitted	Stress-integration tolerance used by the UMAT.
FTOL	all cases	Optional; UMAT default if omitted	Yield-surface tolerance used by the UMAT.
LTOL	all cases	Optional; driver default if omitted	Driver loading tolerance used when enforcing the target path.
nSteps	all cases	Required in packaged cases	Number of imposed loading increments.
dEpsAxial	all cases	Required in packaged cases	Axial strain increment applied at each step.
VoidRatio	all cases	Required in packaged cases	Initial void ratio used by the standalone driver and the hydraulic update.

Input key	Used by	Required / choices / defaults	Meaning
StressXX, StressYY, StressZZ	all cases	Required in packaged cases	Initial total stress components. The packaged cases use an isotropic starting state.
InitialPoreAirPressure, InitialPoreWaterPressure	QOverPnet, ConstWContent	Required for unsaturated modes	Starting pore-air and pore-water pressures. The mini computes suction as $s = u_a - u_w$, so these two entries define the initial suction together. For example, 0 and -100 mean $s = 100$ kPa, while 0 and 0 give $s = 0$.
VG_n, VG_m	QOverPnet, ConstWContent	Required for unsaturated modes	Shape parameters of the hysteretic van-Genuchten-type SWRC used by the mini.
Pd, Pw	QOverPnet, ConstWContent	Required for unsaturated modes	Drying and wetting pressure scales used in the hysteretic retention update.
OmegaPrime	QOverPnet, ConstWContent	Required for unsaturated modes	Coupling parameter that links suction evolution to void-ratio changes in the retention model.
chi_b1, chi_b2	QOverPnet, ConstWContent	Required for unsaturated modes	Parameters of the Bishop-type $\chi(S_w)$ weighting used in the effective-stress calculation and therefore in p_{net} .

Input key	Used by	Required / choices / defaults	Meaning
b_w , b_d , b_sc , alpha_p_c	QOverPnet, Const WContent	Required for unsaturated modes with evolving retention state	Scanning-curve and branch-blending parameters for the hysteretic SWRC. alpha_p_c sets the initial position between the main wetting and drying branches.

1.8.3 Hydromechanical assumptions

The standalone implementation makes the following assumptions explicit:

- suction is defined from the prescribed initial pore pressures as $s = u_a - u_w$
- the packaged unsaturated examples use `InitialPoreAirPressure = 0` kPa and `InitialPoreWaterPressure = -100` kPa, so the initial suction is 100 kPa
- the air phase is held constant during the run, so changes in suction come from the water-pressure update only; this corresponds to a vented or fixed-reference air boundary in the standalone mini
- the effective-stress weighting uses the [\chi\(S_w\) function](#) implemented in the mini driver, controlled by `chi_b1` and `chi_b2`
- saturation changes are driven by a hysteretic scanning SWRC, not by a single main drying curve only

For the packaged unsaturated paths, the hydromechanical ingredients are:

- main drying / wetting retention branches controlled by `VG_n`, `VG_m`, `Pd`, and `Pw`
- scanning-curve memory controlled by `b_w`, `b_d`, `b_sc`, and `alpha_p_c`
- coupling between suction and void ratio through `OmegaPrime`
- effective stress through the saturation-dependent [\chi\(S_w\)](#) weighting

So the unsaturated Mohr mini should be read as a mechanical Mohr-Coulomb model paired with a standalone hysteretic retention update and a saturation-weighted effective-stress law.

1.8.4 Sample input

The packaged cases share the same mechanical parameter block and differ mainly in Mode and the hydraulic keys.

Drained triaxial example Path: [mini_tools/MohrRounded/cases/drained/input.txt](#)

```
Mode Drained
E 10000
nu 0.30
Cohesion 10
FrictionAngle 30
DilationAngle 0
Rf 0.10
STOL 1e-3
FTOL 1e-4
LTOL 1e-6
nSteps 300
dEpsAxial -1e-4
VoidRatio 0.40
StressXX -100
StressYY -100
StressZZ -100
```

This is the saturated reference path. It isolates the rounded Mohr-Coulomb response without suction evolution.

Undrained triaxial example Paths:

- [mini_tools/MohrRounded/cases/undrained/input.txt](#)
- [mini_tools/MohrRounded/cases/undrained_dilation5/input.txt](#)

```
Mode Undrained
E 10000
nu 0.30
Cohesion 10
FrictionAngle 30
DilationAngle 0
Rf 0.10
STOL 1e-3
FTOL 1e-4
LTOL 1e-6
nSteps 300
dEpsAxial -1e-4
VoidRatio 0.40
StressXX -100
StressYY -100
StressZZ -100
```

```

Mode Undrained
E 10000
nu 0.30
Cohesion 10
FrictionAngle 30
DilationAngle 5
Rf 0.10
STOL 1e-3
FTOL 1e-4
LTOL 1e-6
nSteps 300
dEpsAxial -1e-4
VoidRatio 0.40
StressXX -100
StressYY -100
StressZZ -100

```

These are saturated constant-volume reference paths. They use the same material parameters and initial stress state as the drained case, but the driver enforces zero total volumetric strain by setting the two radial strain increments to -0.5 dEpsAxial . The only difference between the two packaged undrained cases is the dilation angle:

- undrained/input.txt:DilationAngle = 0
- undrained_dilation5/input.txt:DilationAngle = 5

Constant-suction q/p_net example Path: [mini_tools/MohrRounded/cases/qoverpnet/input.txt](#)

```

Mode QOverPnet
E 10000
nu 0.30
Cohesion 10
FrictionAngle 30
DilationAngle 0
Rf 0.10
nSteps 300
dEpsAxial -1e-4
VoidRatio 0.40
StressXX -100
StressYY -100
StressZZ -100
InitialPoreAirPressure 0
InitialPoreWaterPressure -100

```

```

VG_n 0.28
VG_m 0.98
Pd 98
Pw 196
OmegaPrime 10.6
chi_b1 1.0
chi_b2 0.0
b_w 5.0
b_d 5.0
b_sc 25.0
alpha_p_c 0.5

```

This case keeps suction fixed while driving a triaxial path with approximately $dq / dp_{net} = 3$.

More explicitly:

- `InitialPoreAirPressure 0` and `InitialPoreWaterPressure -100` define an initial suction of 100 kPa
- because this is the `QOverPnet` mode, that suction is then held constant during the loading path
- the stress path is therefore controlled in terms of p_{net} , not just total mean stress
- `VG_n`, `VG_m`, `Pd`, `Pw`, and `OmegaPrime` define the hysteretic SWRC used to evaluate saturation changes consistently with the current void ratio
- `chi_b1 = 1.0` and `chi_b2 = 0.0` reduce the effective-stress weighting to the classical Bishop choice $\chi = S_w$

Constant-water-content example Path: mini_tools/MohrRounded/cases/const_wcontent/input.txt

```

Mode ConstWContent
E 10000
nu 0.30
Cohesion 10
FrictionAngle 30
DilationAngle 0
Rf 0.10
nSteps 300
dEpsAxial -1e-4
VoidRatio 0.40
StressXX -100
StressYY -100
StressZZ -100

```

```

InitialPoreAirPressure 0
InitialPoreWaterPressure -100
VG_n 0.28
VG_m 0.98
Pd 98
Pw 196
OmegaPrime 10.6
chi_b1 1.0
chi_b2 0.0
b_w 5.0
b_d 5.0
b_sc 25.0
alpha_p_c 0.5

```

This case couples the mechanical path with suction and saturation changes while keeping water content fixed.

1.8.5 Output files and columns

The packaged driver writes `stress_results.csv` for all cases and, for the hydraulic paths, also writes `hydraulic_paths.csv` and `X_vs_Sw_suction_e.csv`.

Output file	Produced by	Main use
<code>stress_results.csv</code>	all cases	Main step-by-step mechanical and hydraulic history used by the mini plots.
<code>hydraulic_paths.csv</code>	hydraulic cases	Auxiliary hydraulic history for the unsaturated path plots.
<code>X_vs_Sw_suction_e.csv</code>	hydraulic cases	Effective-stress variable X, saturation, suction, and void-ratio history in one table.

Main columns in `stress_results.csv`:

Output column	Meaning
<code>step</code>	Load-step index written by the standalone driver.
<code>exx, eyy, ezz, ezy, ezx, exy</code>	Strain components for the accepted step state.

Output column	Meaning
sxx, syy, szz, szy, szx, sxy	Stress components for the accepted step state.
q	Deviatoric stress measure used in the triaxial plots.
p	Mean stress measure reported by the driver.
pnet	Net mean stress used for the q-p _{net} plots. In the saturated drained and undrained cases, this is the same as p because suction is inactive.
Sw	Degree of saturation.
suction	Suction computed from the pore-pressure update.
e	Void ratio.

The plots in the next section are generated from these packaged case CSVs.

1.9 Results

The plots below are produced directly from the packaged case directories discussed above. All bundled cases use $E = 10$ MPa, $\nu = 0.30$, $c = 10$ kPa, $\phi = 30$ deg, $\psi = 0$ deg, $R_f = 0.10$, $e_0 = 0.40$, and the same initial isotropic total stress state $Stress_{XX} = Stress_{YY} = Stress_{ZZ} = -100$ kPa.

1.9.1 Drained reference case

Bundled inputs:

- [mini_tools/MohrRounded/cases/drained/input.txt](#)
- [mini_tools/MohrRounded/cases/drained_dilation5_nocap/input.txt](#)
- [mini_tools/MohrRounded/cases/drained_dilation5_cap/input.txt](#)

Left: deviatoric response of the saturated drained triaxial path. Right: the corresponding stress path in q-p_{net} space for the same packaged drained input.

Left: drained comparison for the two additional packaged cases with $DilationAngle = 5$, one without a dilatancy cap and one with $DilationPvCap = 0.002$. Right: the corresponding void-ratio evolution. The capped case arrests dilation earlier and therefore retains a lower void ratio at the same axial strain.

1.9.2 Undrained reference case

Bundled inputs:

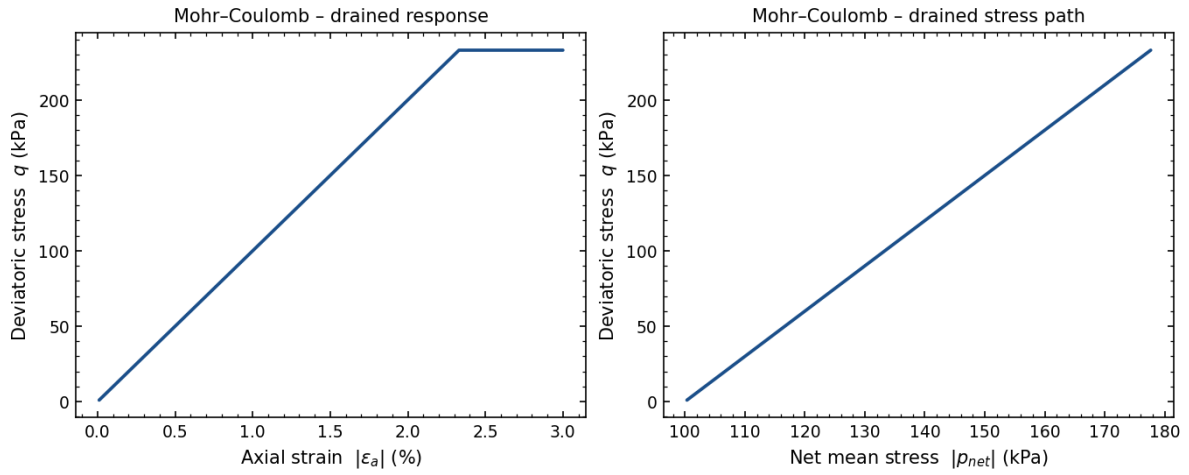


Figure 2: Drained axial response and stress path

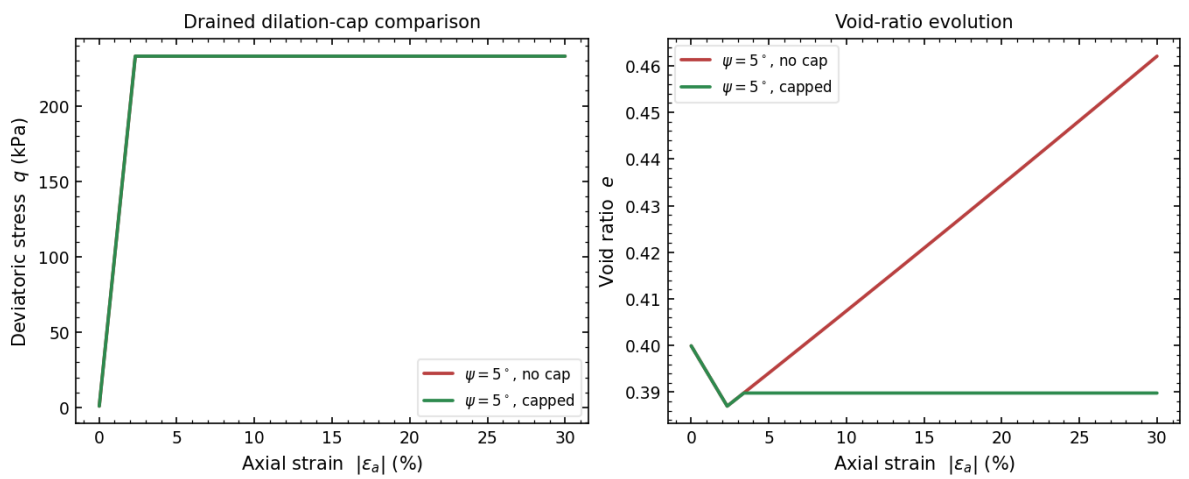


Figure 3: Drained dilation-cap comparison

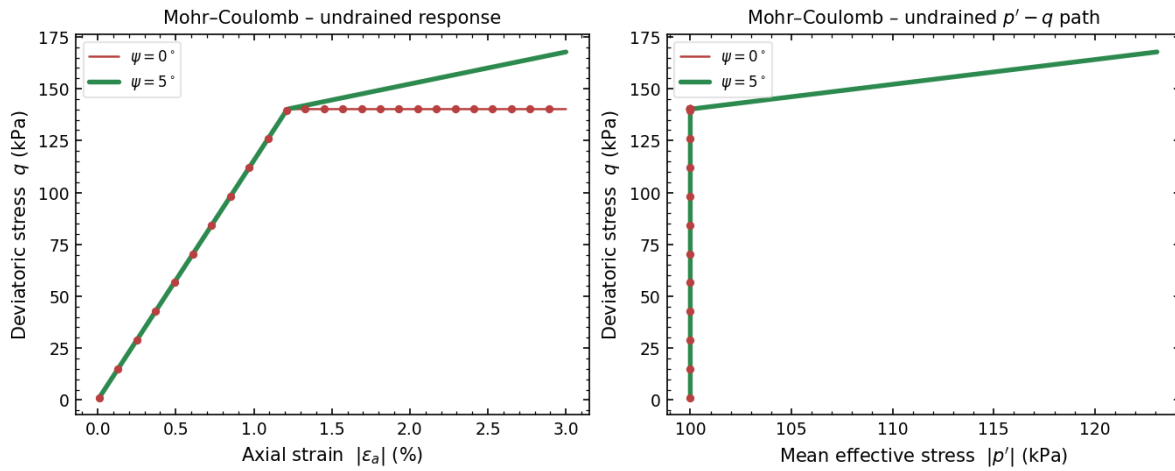


Figure 4: Undrained axial response and stress path

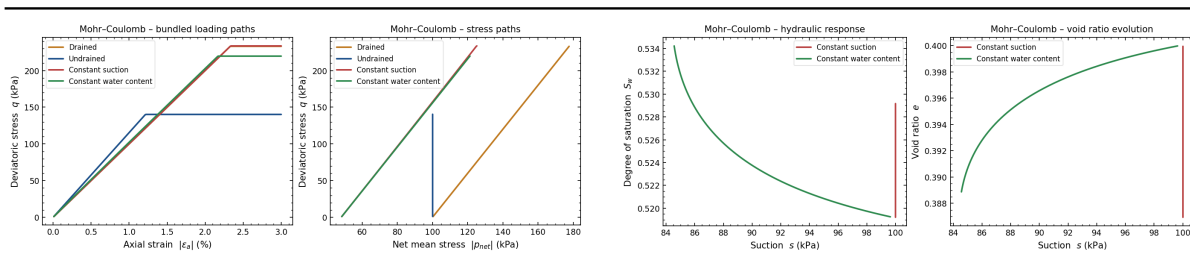
- [mini_tools/MohrRounded/cases/undrained/input.txt](#)
- [mini_tools/MohrRounded/cases/undrained_dilation5/input.txt](#)

Left: deviatoric response of the two saturated undrained triaxial paths. Right: the corresponding $p' - q$ stress paths. The blue curve is the non-dilatant packaged case with Dilation Angle = 0, and the green curve is the companion case with DilationAngle = 5.

1.9.3 Unsaturated companion cases

Bundled inputs:

- [mini_tools/MohrRounded/cases/qoverpnet/input.txt](#)
- [mini_tools/MohrRounded/cases/const_wcontent/input.txt](#)



Left: axial stress-strain response and $q - p_{net}$ stress paths for the drained and undrained saturated reference cases together with the constant-suction and constant-water-content unsaturated paths. Right: hydraulic response of the two unsaturated bundled cases, showing how saturation and void ratio evolve with suction under the two different constraints.

For these two unsaturated examples:

- QOverPnet keeps suction fixed and drives an approximately constant $dq / dp_{net} = 3$ path
 - ConstWContent enforces constant water content, so suction, saturation, and void ratio evolve together during the loading path
-

1.10 Applications and limitations

- Best suited to general frictional soil analyses such as slopes, retaining systems, bearing-capacity checks, and baseline elastoplastic simulations.
 - Can be used in unsaturated analyses when paired with an effective-stress model, but the constitutive law itself is not a suction-hardening critical-state formulation.
 - Not intended to reproduce critical-state hardening, fabric evolution, cyclic mobility, or state-parameter sand behavior.
-



ARTEMIS DEV

1.11 References (selection)

- Abbo, A. & Sloan, S. (1995). *A smooth hyperbolic approximation to the Mohr–Coulomb yield criterion*.
- Ghorbani, J., Nazem, M., Moridpour, S. and Carter, J.P. (2026). *An unsaturated Mohr-Coulomb model with tuneable near-dry suction-driven strength and attenuation: implications for bearing capacity*. Computers and Geotechnics, 191, 107792.